Available online at www.sciencedirect.com

SCIENCE DIRECT®

Coordination Chemistry Reviews 245 (2003) 49–64

COORDINATION CHEMISTRY REVIEWS

www.elsevier.com/locate/ccr

# The supramolecular chemistry of the sulfonate group in extended solids

Adrien P. Côté, George K.H. Shimizu*

*Department of Chemistry, University of Calgary, 2500 University Drive NW, Calgary, Alberta, Canada T2N 1N4*

Received 11 October 2002; accepted 21 February 2003

## Contents

## Abstract

Organosulfonates ($RSO_3^-$) are largely regarded as poor ligands by coordination chemists, and have typically been employed as 'non coordinating' anions in past synthetic and structural work. Indeed, the majority of transition metal aqua complexes with sulfonate counter anions show that the sulfonate group cannot readily displace water from the coordination sphere of the metal ion. There exists a strong structural analogy between the $RSO_3^-$ and the phosphonate $RPO_3^{2-}$ group, a functionality which has been employed with great success in the generation of functional extended architectures. The contrast lies in the fact that individual metal–oxygen interactions with the sulfonate group are weaker, when employed with suitably soft metal cations, but may be employed cooperatively, to still yield a stable solid. This review deals with some of the functional frameworks we have reported which take advantage of the inherent coordinative pliancy of the sulfonate group to generate extended networks. Features of the discussed frameworks include sponge-like guest sorption, anion exchange, and topotactic intercalation.

*Keywords:* Sulfonate; Coordination network; Supramolecular; Self-assembly; Silver; Barium

## 1. Introduction

### 1.1. Extended coordination solids

The concept of an 'organic zeolite', a self-assembled porous solid built from organic molecules, is highly appealing [1–3]. The name conjures images of an extended solid with the functionality of a porous metal oxide (sieve properties, ion exchange, catalysis. . . ) [4–12] yet with the tunability offered by the library of synthetic organic chemistry available to modify the molecular components. Seemingly, functional groups can be appended to the walls of the cavities to alter the polarity of the channels or to form secondary interactions with included species. Efficient enantioselective separations instinctively become more feasible. Another advantage offered by using a network building block derived from molecular, rather than an atomic unit, is that, in principle, larger pore sizes are attainable simply

---

* Corresponding author. Tel.: +1-403-220-5347; fax: +1-403-289-9488.
*E-mail address:* gshimizu@ucalgary.ca (G.K.H. Shimizu).

0010-8545/$ – see front matter © 2003 Elsevier B.V. All rights reserved.
doi:10.1016/S0010-8545(03)00033-X

by employing a larger organic molecule. The shape of void regions may also be adjusted in this manner. The major shortcoming of this organic approach, depending on the proposed application, is certainly the marked lower thermal stability of these solids as they are necessarily sustained by purely non-covalent interactions.

In comparison to a metal oxide framework and a wholly organic assembly, a coordination chemistry approach offers a compromise [13–20]. If we consider an aluminosilicate structure as a starting point for a hypothetical modification, polytopic organic ligands can be considered as replacements for the $O^{2-}$ anions, thus providing the advantages of organic molecules listed above, and other metal ions can take the place of the $Al^{3+}$ and $Si^{4+}$ ions. Incorporation of different metal centers, particularly transition metals, presents further opportunities for tuning the structure not readily offered by either the wholly inorganic or organic approaches [21]. Choice of an octahedral or square planar metal centre incorporates a 90° angle into the structure thus giving more options for defining the shape of a pore. While 109.5 and 120° angles are easily attainable with aluminosilicate units or solely organic molecules, right angles typically are not. Moreover, the electronic properties of the metal center, whether they be related to color, magnetism, luminescence, etc. become part of the extended framework. The metal centers could also be employed as Lewis acid centers for catalytic applications [22], an enticing prospect especially when coupled with a guest selective support framework.

In choosing an approach to construct a zeolite mimic, selecting the latter 'metal–organic' methodology has been met with the most success. Numerous examples have now been reported employing metal–carboxylate or metal–pyridine units to build robust architectures that display permanent porosity [23–27]. The large pores offered in some these compounds have shown considerable potential for gas storage applications [28–30].

In introducing this review on functional networks constructed from sulfonates ($RSO_3^-$) a specific mention and comparison of the networks formed by the phosphonate ($RPO_3^{2-}$) group is merited [31,32]. The phosphonate bears a strong structural analogy to the sulfonate group, in that they are both trioxy anionic units with an organic pendant having local $C_{3v}$ symmetry. The obvious difference being the greater dianionic charge associated with the phosphonate. The phosphonate group has been extensively studied owing to the regularity of its assembly into layered networks with a wide range of pendant R groups. The two-dimensional structures are typically highly robust and can in fact be exfoliated to films [33–38]. This field has recently been thoroughly reviewed by Clearfield [39].

### 1.2. *The sulfonate group*

The coordination chemistry of sulfonate group has, until quite recently, remained relatively unstudied. The reason for this has simply been that sulfonate anions are regarded as poor ligands. Certainly for the majority of transition metal complexes, sulfonate anions are generally considered to be weakly interacting or non-interacting [40]. This notion is particularly true for the trifluoromethanesulfonate (triflate, $^-$OTf) anion. Indicative of the significance of $^-$OTf coordinative tendencies, Lawrence published a review in which the known coordination chemistry was discussed [41]. This pre-eminent perception of sulfonate anions as weakly coordinating though is largely justified based upon the library of transition metal sulfonate crystal structures obtained under hydrous conditions [42–46]. The vast majority of these compounds show a completely hydrated metal ion with the sulfonate functioning as a true non-coordinating counter ion [47,48]. Thompson et al. have published a series of papers dealing with homoleptic sulfonate coordination to transition metals, however this was primarily an infrared investigation that required strict anhydrous conditions [49–52].

As discussed, with most metal ions under hydrous conditions, sulfonate ions do not efficiently displace solvent from the primary coordination sphere. Exceptions to this statement are alkali ions, larger alkaline earth ions, and silver(I). The common feature of these ions is that none of them have stringent preferences with respect to coordination number or geometry. In our research group, our realization of these coordinative possibilities began with the structural elucidation of the silver *p*-toluenesulfonate [53] and silver benzene sulfonate structures [54]. Both of these compounds have layered structures, reminiscent of metal phosphonate analogues, but in stark contrast to metal phosphonates, minor changes in the nature of the R group on the sulfonate result in a change in the bridging mode of the anion. For example, in silver *p*-toluene sulfonate, each $SO_3$ group bridges five metal centers, while for silver benzene sulfonate six metal centres are bridged. Fig. 1 shows a comparison of the layer structures of AgOTs and $AgPhSO_3$.

Upon examining the connectivity of AgOTs and $AgPhSO_3$ structures, the important role of cooperative interactions in the formation of these and other extended structures becomes evident. Quite robust infinite solids can be generated based upon interactions which individually would be regarded as not particularly strong. In effect, it is simply not possible to break individual bonds, a great many bonds must be broken simultaneously [55]. With regards to the coordination chemistry of the sulfonate group, this factor is particularly significant as it applies both to a single sulfonate group and to polysulfonated ligands (vide infra). The thermal stability of layered silver sulfonate salts to up to 353 °C is a reflection strength of the cooperativity observed in metal–sulfonate aggregation patterns [54].

For a single sulfonate group, while each individual metal–oxygen atom interaction is weaker, each oxygen atom has the potential to bridge more than one metal center. While formally a single sulfonate oxygen atom can bond to three metal centers, more typically, the oxygen atoms of a sulfonate group will bridge a maximum to two metal ions. Fig. 2 shows a sampling of some of the possible coordi-

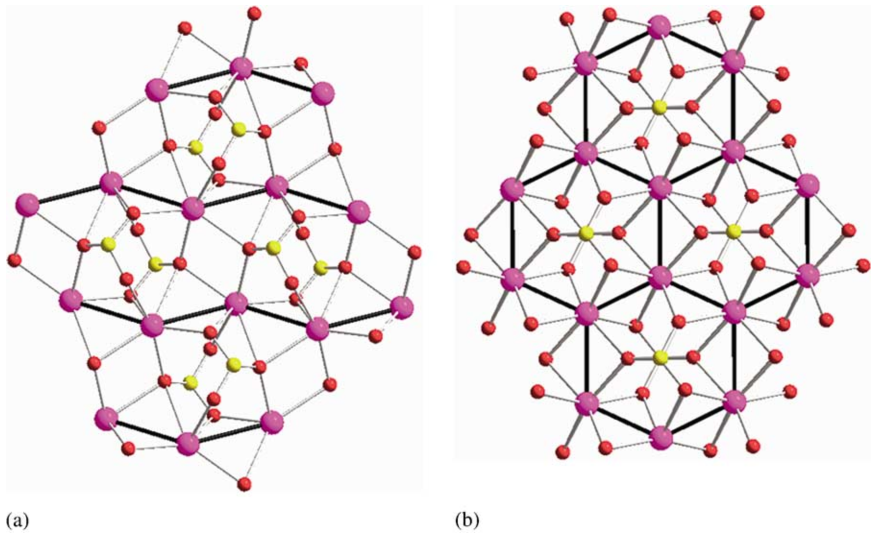

Fig. 1. Comparison of the sulfonate bridging modes in (a) AgOTs and (b) $AgSO_3Ph$.

nation modes for the sulfonate group. We have observed a maximum of six metal centers bridged by a single sulfonate group as observed in the $AgPhSO_3$ structure [54].

The large bridging numbers like the $\mu^5$ and $\mu^6$ modes observed in AgOTs and $AgPhSO_3$ are unattainable with other commonly employed classes of ligands such as carboxylates and pyridines. Notably, whereas the ligating directionality of a pyridine or a carboxyl group is confined to a plane, the spherical shape of the electron density that encompasses a sulfonate group allows metal coordination to an additional dimension, serving to further increase the connectivity of the network and favour the formation of a robust structure. This coordinative flexibility in terms of bridging modes, combined with the roughly spherical shape of the $SO_3$ unit, has led us to draw the analogy between a sulfonate group and a 'Ball of Velcro' [56].

In addition to the multiple bridging modes possible for a sulfonate group, a more obvious means of using cooperative bonding interactions is to simply have more than one sulfonate group on a ligand. An important factor in considering the previous works on metal sulfonates is that the majority of these complexes dealt with simple monosulfonate anions, although recently, Cai et al. have reported studies on the coordinating preferences of some disulfonate anions with various metal ions in the presence of other stronger ligands [57–61]. Multiply sulfonated ligands have much greater potential to form a higher dimensional, and hence more stable structure. Atwood and Raston have independently used metal ions in primary and secondary sphere roles to assemble sulfonated calix[4]- and calix[5]arenes [62–68]. These works illustrate the utility of polysulfonated ligands to form multidimensional, usually layered, structures and have been reviewed elsewhere [69].

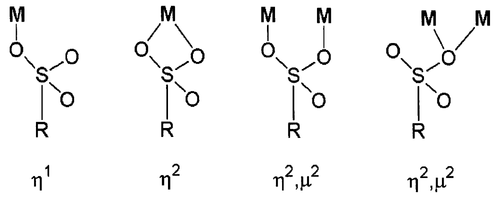

Fig. 2. Possible coordination modes for sulfonate anions in the solid-state. Combinations of these coordination modes also occur for a single $SO_3$ group.

### 1.3. *Scope of review*

This review will provide an overview of some of the recent work in our group in the context of the topics discussed above. Examples will be presented which show that sulfonate ions can be employed to not only generate highly robust and functional architectures, but also 'softer' networks whose properties are best described as sponge-like. This latter class of compounds represents a divergence from traditionally held notions that functional properties can only be imparted to extended solids that exhibit permanent porosity. As will be shown, a structurally pliant solid may still possess function and, in fact, offers opportunities not possible in more rigid networks.

## 2. Rigid and robust sulfonate frameworks with $Ba^{2+}$ ions

$Ba^{2+}$ ions have a large radius (Pauling ionic radius = 1.35 Å) and are typically observed to have irregular geometries [70]. These properties combine to allow for a soft cation with a lower affinity for aqua ligands. With respect to the coordination of a sulfonate group, $Ba^{2+}$ ions provides a coordinatively accessible cation, in both a substitutional and geometrical sense. Moreover, the doubly positive charge on the metal ion versus the monoanionic charge on a sulfonate group would necessarily mean that, with the appropriate ligands, a higher degree of intermolecular aggregation would occur to maintain a charge balance. This choice of ligand could also then provide the opportunity to generate void space within the solid.

### *2.1. Gas sorption in a pillared metal sulfonate network*

Our first example of a functional sulfonate coordination network arose from the preparation of the barium salt of 4,5-dihydroxybenzene-1,3-disulfonate (**1**), which presented a pillared layered structure having the formula $\{Ba[(\mathbf{1})(H_2O)]\cdot H_2O\}^\bullet$ (Fig. 3) [71].

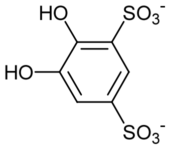

**1**

Here we drew another contrast to layered metal phosphonates. Attempts to generate void space by using a diphosphonate ligand as a pillar to bridge layers, leads to the formation of a dense structure where the ligands become close packed. In order to generate a porous solid in these systems, a mixture of a diphosphonate pillar and a monophosphonate with a small R group is required to generate an alternating sequence of pillars and spacers between the layers [72–74]. Unfortunately, the ordering of pillars and spacers in these structures tends to be random, and this lack of ordering results in a non-uniform distribution of pore sizes throughout the network. Our disulfonate ligand **1** can be regarded as being a 'bent pillar', whereby a microporous network is predisposed to form owing to the dissymmetric nature of the ligand. The network does not pack efficiently in the solid-state and compensates by including water within the interlayer region in ∼4 Å diameter channels. Scheme 1 illustrates these three different possibilities for the pillaring of layered networks. Indeed, if a linear disulfonate ligand is employed, dense structures are also obtained [75–77]. However, with phosphonate groups, the option to simply alter the geometry of functional groups on a ligand while retaining a layered structure would not be as facile due to the more rigid coordinative demands of the $PO_3$ group. The 4,5-diol moiety of **1** plays an important role by further anchoring the ligand to the layer and directing the 1,3-$SO_3$ groups to oppose each other as illustrated in Scheme 1.

The aggregation pattern of $\{Ba[(1)(H_2O)]\cdot H_2O\}^\bullet$ is complex with 1 coordinating to six different barium centers and each barium in turn being nine-coordinate with an irregular geometry. The coordination sphere is comprised of six sulfonate oxygen atoms, from five different sulfonate groups, the catechol oxygen atoms which coordinate in a doubly protonated form, and a water molecule that projects into the interlayer. The highly crosslinked nature of the this network results in a very robust solid that is stable to >400 °C, clearly illustrating that solids generated with a coordinatively flexible building blocks are not compromised by poor structural stability. This is further illustrated by the capability of $\{Ba[(1)(H_2O)]\cdot H_2O\}^\bullet$ to reversibly sorb hydrogen sulfide and water. Heating a bulk sample of $\{Ba[(1)(H_2O)]\cdot H_2O\}^\bullet$ to 110 °C for 10 min selectively removes the water molecules that exist in the channels without altering the structure as confirmed by PXRD analysis. This leaves empty channels imprinted with the shape of the guest water molecules. When the atmosphere exposed to the empty network $\{Ba[(\mathbf{1})(H_2O)]\}^\bullet$ is changed to a flow of $H_2S$ or humid $N_2$ their uptake can be measured gravimetrically. With respect to an equivalent of displace $H_2O$, 0.93 equivalents of $H_2S$, and near quantitative uptake of $H_2O$ is observed. The network is also selective, and rejects other small molecules such as $H_2$, $O_2$, $Cl_2$, $SO_2$, $CO_2$, Ar, MeOH, and $CH_4$ [78]. The latter substrate is of specific importance to the petroleum industry where abatement of sour gas, largely comprised of $H_2S$ and $CH_4$, is of particular concern. Indeed $\{Ba[(\mathbf{1})(H_2O)]\}^\bullet$ can sorb $H_2S$ from a mixed atmosphere of $CH_4$ and $H_2S$. From a synthetic standpoint, the preparation of $\{Ba[(1)(H_2O)]\cdot H_2O\}_\circ$ is extremely facile. Phase pure, and functional, polycrystalline $\{Ba[(\mathbf{1})(H_2O)]\cdot H_2O\}^\bullet$ is obtained in one step from the commercially available sodium salt when equimolar aqueous solutions of $Na_2\mathbf{1}$ and $BaCl_2$ are mixed, resulting in a metathesis reaction where the barium network spontaneously precipitates from solution in 95% yield.

### *2.2. Anion exchange in a robust barium coordination network using a trisulfonate ligand*

The ligand used in this study was the pseudo-trigonally symmetric trisulfonate ligand 1,3,5-tris(sulfomethyl)-benzene (**2**). The design of this ligand, based on a mesitylene core, was rationalized on the expectation that the organic groups would not be able to pack efficiently in two dimensions upon coordination in the solid state. Moreover, the spherical shape of the sulfonate group would enable the coordinating ability of **2** to extend beyond two dimensions.

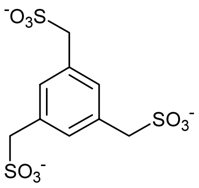

**2**

Upon complexation of **2** with $BaCl_2$, the highly robust network of the formula $\{Ba_2[(\mathbf{2})(H_2O)_5]Cl\}^\bullet$ was obtained, with the same synthetic ease and efficiency as for the preparation of $\{Ba[(\mathbf{1})(H_2O)]\cdot H_2O\}^\bullet$ (Fig. 4) [79]. The resultant structure also has a pillared layered motif despite the greater spatial divergence of the $SO_3$ groups in **2** as compared to **1**. The most significant feature of $\{Ba_2[(2)(H_2O)_5]Cl\}^\bullet$ is

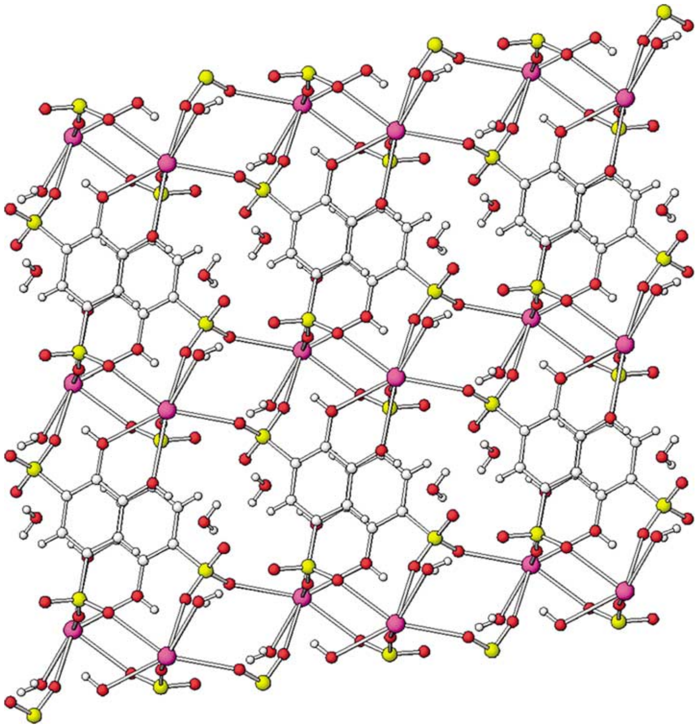

Fig. 3. Extended structure of $\{Ba[(\mathbf{1})(H_2O)]\cdot H_2O\}^{\bullet}$ showing the water filled channels in the pillared interlayer region.

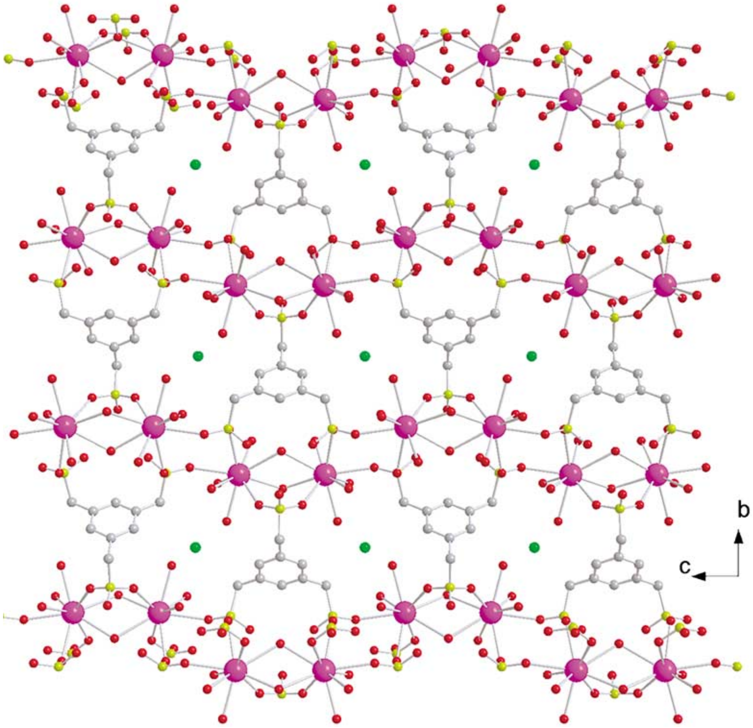

Fig. 4. Extended structure of $\{Ba_2[(\mathbf{2})(H_2O)_5]Cl\}^{\bullet}$ showing the chloride containing channels running along the crystallographic *a*-axis.

the inclusion of chloride anions in channels running through the interlayer region, resulting in an anti-zeolitic cationic framework.

Upon heating, $\{Ba_2[(\mathbf{2})(H_2O)_5]Cl\}^{\bullet}$ undergoes minor structural contraction ( $< 3\%$) upon loss of coordinated water but retains its phase and crystallinity until decomposion at 420 °C. The stability of this network is also demonstrated by its very low solubility. Ultimately hydrothermal conditions were required in order to convert polycrystalline 'as synthesized' material to single crystals.

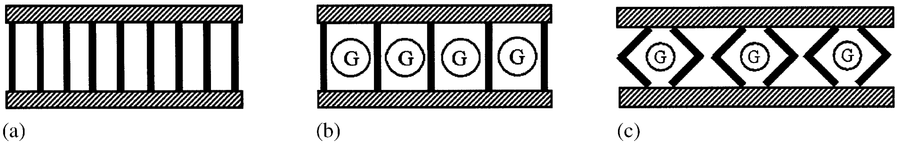

Scheme 1. Pillaring of layered networks showing (a) close packing of linear pillars with no void space; (b) alternating pillars and small R-groups to generate porosity; (c) use of 'bent' pillars to creat pores with a single type of R group.

It is somewhat unexpected that this material, particularly the solid obtained at ambient conditions, would incorporate both **2** and chloride anions given the high insolubility of other 'homo-anionic' barium organosulfonate networks. This is a strong indication of the stability of the cationic skeleton. The observation of mixed ions is also rare in phosphonate chemistry. We are aware of only a few examples where this is the case and these actually incorporate cationic viologen pillars [80,81]. The overall structure of $\{Ba_2[(\mathbf{2})(H_2O)_5]Cl\}^{\bullet}$ can be described as ruffled layers of $SO_3$-bridged $Ba^{2+}$ ions, 'pillared' by the mesitylene core of **2** to generate the chloride containing channels. The dimensions of the channels are approximately 9.1 × 7.9 Å, which translates to 5.1 × 6.7 Å when van der Waals radii are considered (cf. van der Waals radius of $Cl = 1.75$ Å). Water molecules in the structure are coordinated to $Ba^{2+}$ and form long hydrogen bonds with the $Cl^-$ ions. The ligand adopts a *cis–cis–trans* conformation with respect to the orientation of the methylenesulfonate groups and the central ring, giving **2** a roughly chair-like profile. Again a highly crosslinked network is obtained and overall **2** bridges ten $Ba^{2+}$ centers.

The ion exchange capabilities of this network were examined. In the presence of one equivalent of fluoride ion, a 75–80% exchange of the chloride ions is achieved. This was confirmed by gravimetric analysis, PXRD, $^{19}$F-NMR spectroscopy, C, H, Cl, F elemental microanalysis, which also discounted the potential formation of $BaF_2$. Anion exchange in coordination networks is rare, and generally occurs only if a large excess of the new anion is present [82–87]. To our knowledge the exchange in $\{Ba_2[(\mathbf{2})(H_2O)_5]Cl\}^{\bullet}$ is the most facile exchange reported in a coordination network to date. The affinity of $\{Ba_2[(\mathbf{2})(H_2O)_5]Cl\}^{\bullet}$ for $F^-$ is surprising; whereas the bromide analogue is easily attained using an analogous preparation using $BaBr_2$, the fluoride analogue of cannot be synthesized starting with $BaF_2$. This result further corroborates the stability of the cationic framework in $\{Ba_2[(\mathbf{2})(H_2O)_5]Cl\}^{\bullet}$.

The mechanism for ion exchange was proposed to occur from the two-way passage of ions in the channels of $\{Ba_2[(\mathbf{2})(H_2O)_5]Cl\}^{\bullet}$. Conducting the exchange in $D_2O$, it was observed that 20% of the water in the structure is ejected during exchange. Thus the aquo ligands are labile, and mobile within the channels. Given that the van der Waals radii for $Cl^-$ and $F^-$ are 1.75 and 1.47 Å, respectively, a minimum channel breadth of 6.44 Å is required for two-way passage. Recalling the channel dimensions were 5.09 × 6.71 Å, this is apparently too small to accommodate such an arrangement. As shown in Fig. 5, the passage of $Cl^-$ and $F^-$ need not occur on a line between the two nearest transannular barium centres. A more likely mechanism has the two ions passing along a line defined by two Ba centers laterally displaced down the channel. This is a distance of 10.37 Å, which converts to 6.37 Å when van der Waals radii are considered. Comparing this value with the effective channel dimensions shows that an additional 0.07 Å is required for a two-way passage of ions. This additional space is easily accommodated for the anions residing in small pockets and dips that exist between adjacent $Ba^{2+}$ ions.

### 2.3. Other dimensions: a 1D-barium sulfonate network

Previously, it has been generally preconceived that all Ba sulfonates are layered networks and, on this basis, these compounds have found considerable use as lubricants [88]. We have found that this is not the case as evidenced by the 1D network $\{[Ba(\mathbf{3})_2(H_2O)_4]\cdot EtOAc_{0.5}\}^{\bullet}$ which results upon crystallization of 2-pyridine ethanesulfonate (**3**) with $Ba^{2+}$ from water/ethylacetate [89]. The complex is composed of inorganic Ba–$SO_3$ columns with pendant pyridylethane groups which serve to define hydrophobic channels capable of organic guest inclusion (Fig. 6).

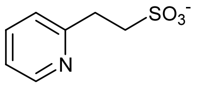

**3**

Although this framework irreversibly collapses to a 2D structure (PXRD) upon heating and loss of EtOAc guests, it serves to exemplify that a corollary to coordinative flexibility is greater structural diversity. As there are no π–π stacking interactions in this structure, the 1-dimensional motif is entirely 'supported', or driven, by van der Waals and weak hydrogen bonding interactions between the columns and guest EtOAc. This suggests that, not only may the coordination motif of a sulfonate network be strongly governed by ligand preorganization, but also the role of guest templation in metal–sulfonate aggregation patterns is also quite significant.

## 3. Flexible sulfonate frameworks with $Ag^+$ or $Ba^{2+}$ ions

Silver(I) cations are renowned for having pliant coordination spheres due primarily to their $d^{10}$ electronic config-

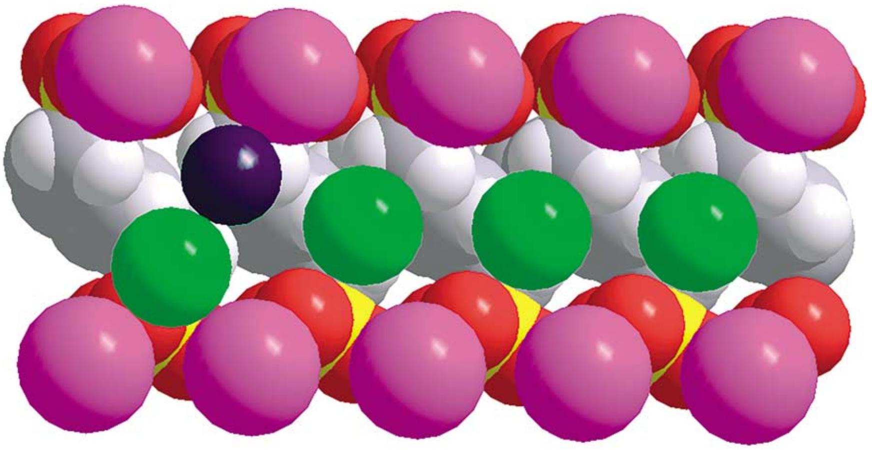

Fig. 5. Space-filling representation, at van der Waals distances, of $\{Ba_2[(\mathbf{2})(H_2O)_5]Cl\}^{\bullet}$, showing a cross-section of a single channel. The figure depicts the two-way passage of $Cl^-$ and $F^-$ ions within the confines of each channel. As the water molecules are labile they are not included in the picture.

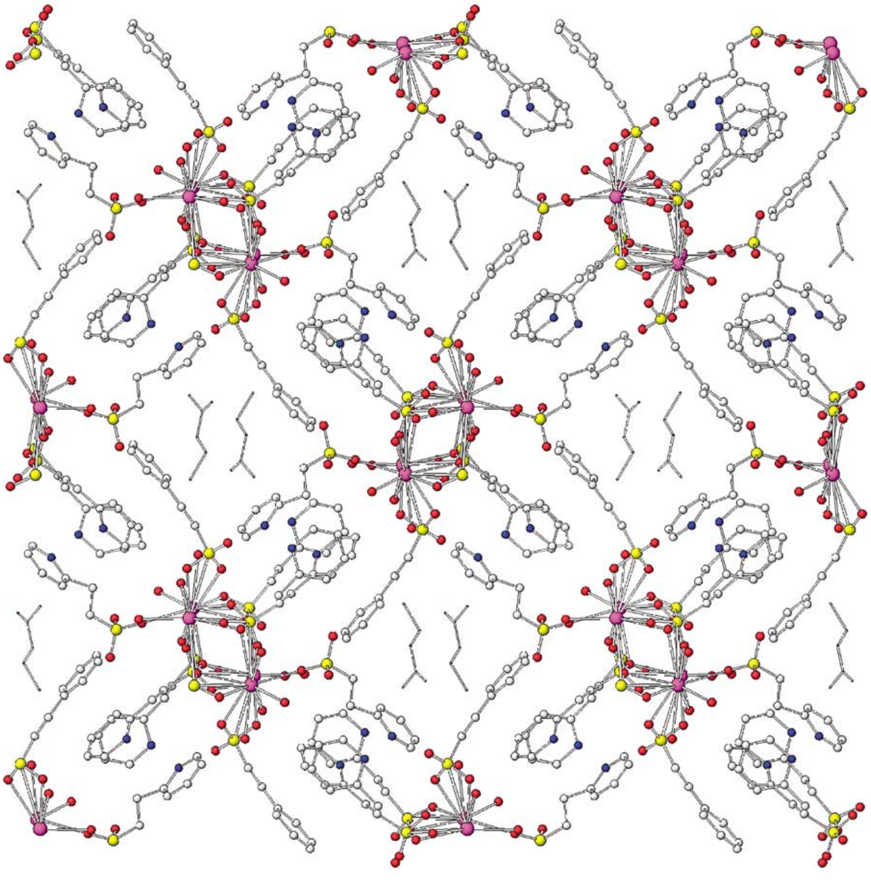

Fig. 6. View down the *a*-axis of $\{[Ba(\mathbf{3})_2(H_2O)_4]\cdot EtOAc_{0.5}\}^{\bullet}$ showing the orientations of the 1D columns in the structure and the hydrophobic EtOAc filled channels which run parallel.

urations [90]. Coordination numbers from two to nine have been observed, often with distorted coordination geometries owing to the inherent lack of ligand field stabilization effects. Along with its soft Lewis acidic properties, $Ag^I$ ions are a particularly good match for the flexible coordinative tendencies of sulfonate anions. This unique combination leads to networks that are readily capable of rearrangements that, in turn, can lead to their adaptive responses towards external stimuli from guest molecules. Barium cations can also act in this respect, but owing to their harder Lewis acidity water tends to also be incorporated within their coordination spheres. In this light, often a sulfonate network's function can be defined by the structural transformations it undergoes.

### *3.1. A sponge-like luminescent coordination framework*

An Aufbau approach was used to assemble the porous luminescent network $\{Ba_2(H_2O)_4[Eu4_3(H_2O)_2](H_2O)_{5.44}Cl\}^{\bullet}$ by taking advantage of the differences in the Lewis basicity of the sulfonate and *N*-oxide components of 4,4′-disulfo-2,2′-bipyridine-*N*,*N*′-dioxide (**4**) [91].

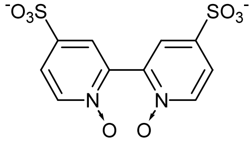

**4**

Chelation of $Eu^{3+}$ via the hard *N*-oxide oxygen donors of 4 results in a discrete complex in which the sulfonates are directed outwards from the Eu center. Using this now sulfonate functionalized Eu complex as a ligand, this building block was then cross-linked through the $SO_3$-groups via interactions with $BaCl_2$ (Fig. 7).

The crystallized network forms a three-dimensional framework, consisting of a columnar motif of Ba–$SO_3$ interactions that organize the Eu centres along the crystallographic *b*-axis (Fig. 8). The channels that run along the *c*-axis as shown in Fig. 7, having dimensions of approximately 12.49 × 9.84 Å as defined by the shortest *trans*-channel metal–metal distances. These values convert to ~8.5 × 5.8 Å when van der Waals radii are taken into account. Uncoordinated water molecules, ~5.5 per Eu center as modeled crystallographically, occupy the channels. Chloride anions (not seen in Fig. 8) exist in small ‘grottos’ off the axis of the channels behind the Eu centers and form hydrogen bonds with coordinated water molecules from Ba and C–H hydrogen bonds with the α-protons of **4**. Coordinated water molecules projecting into the channels from both Eu and Ba centres define a *trans*-channel distances of 8.41 and 5.34 Å. Due to the lability of these aquo ligands the former channel dimensions were chosen (vide supra).

The $\{Ba_2(H_2O)_4[Eu4_3(H_2O)_2](H_2O)_{5.44}Cl\}^{\bullet}$ is a hybrid structure and adopts some of the features presented in earlier networks. The columnar Ba–$SO_3$ aggregation is observed, albeit of a different coordination motif, is now forms part of a three dimensional structure using a properly designed building block This structure also displays a high degree of aggregation between $Ba^{2+}$ ions and sulfonate anions, the two types of Ba centers crosslink four and five $[Eu4_3(H_2O)_2]^{3-}$ building blocks, respectively. The $\{Ba_2(H_2O)_4[Eu4_3(H_2O)_2](H_2O)_{5.44}Cl\}^{\bullet}$ structure also exhibits both solvent and anion inclusion.

In keeping with the analogy of the sulfonate group acting as a ‘Ball of Velcro’ [56], $\{Ba_2(H_2O)_4[Eu4_3(H_2O)_2]$-$(H_2O)_{5.44}Cl\}^{\bullet}$ exhibits sponge-like sorption behavior. Thermogravimetric analysis of this network showed a steady mass loss to 105 °C corresponding to loss of both free and coordinated water molecules. The sample is then stable to 320 °C. A PXRD analysis revealed that the sample becomes amorphous after dehydration, indicating that the network collapses, but not totally as a small internal surface area remains (15.3 $m^2\ g^{-1}$). Upon reintroduction of water vapour, the PXRD pattern remains amorphous, however TGA data revealed that, in fact, the network resorbs > 95% of the lost solvent, a value that requires the uptake of both coordinated and free $H_2O$. The sorption/desorption cycle can be repeated with > 95% efficiency. The fact that the solid does not completely revert to its nascent form with each cycle is sufficient to yield the observed amorphous PXRD pattern.

One of the primary rationales for a coordination chemistry approach to generating extended solid networks is not only the prospect for greater structural diversity, but also for the incorporation of unique functional features [13–18]. So, in addition to its structural role, the $Eu^{3+}$ ions in the network also impart luminescent properties. The expected red luminescence ($\lambda_{exc} = 464$ nm, $\lambda_{em} = 612$ nm) of a $Eu^{3+}$ coordination complex is observed [92–95]. Investigation into the solvent dependence of the luminescence has initially shown that the intensity of the hypersensitive $^5D_0$ to $^7F_2$ transition decreases ~50% in the absence of water and ~70% in the presence of nitrobenzene.

### *3.2. Highly selective guest uptake imparted by a tetragonal to triclinic shift in the solid-state*

3-Pyridinesulfonic acid (**5**) was used in this work to form networks incorporating a combination of both strong Ag–pyridine interactions via *N*-coordination and weaker Ag–sulfonate interactions [56].

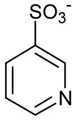

**5**

Extended networks based on pyridine ligands with $Ag^I$ most consistently give a 2:1 linear coordination mode about the metal center [96–100], while as presented earlier, silver salts of monosulfonates generally form layered structures [53,54]. Therefore, for ligand **5**, there exists a competition between two recognized structural motifs. If the linear coordination of pyridine groups were to be observed, only a single other silver ion could be present to interact with two pendant sulfonate groups. This would exclude the possibility for the formation of a layered structure as the required 1:1 silver sulfonate ratio seen in AgOTs and $AgPhSO_3$ is not available. The result is an alternative framework that arises from the interplay between these two competing structural motifs.

Initially we formed the network $[Ag(\mathbf{5})(MeCN)_{0.5}]^{\bullet}$, which is comprised of linked 24-membered rings (Fig. 9). Here the expected linear coordination geometry about $Ag^I$ is observed defining the top and bottom borders of each

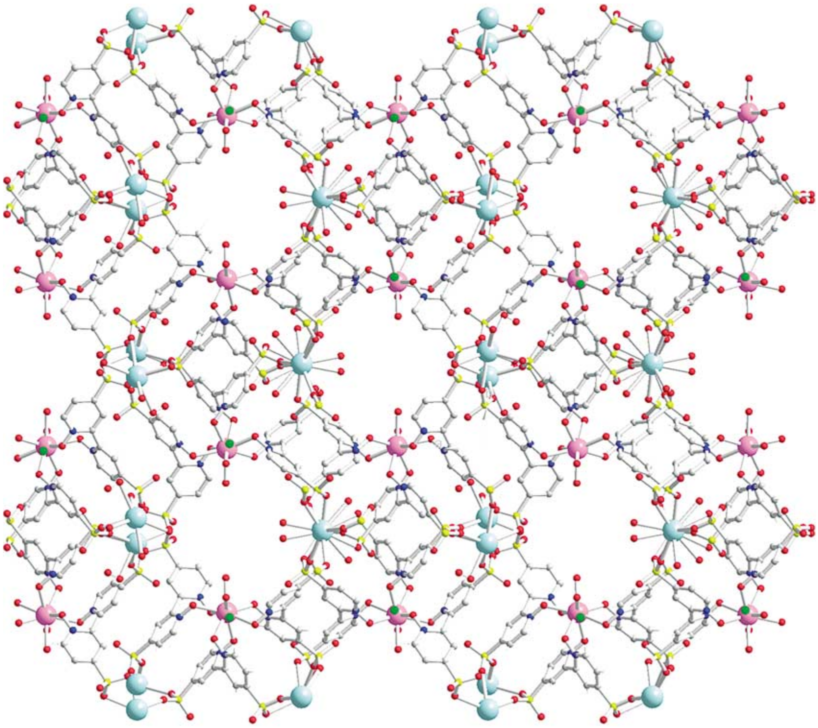

Fig. 7. Extended structure of $\{Ba_2(H_2O)_4[Eu4_3(H_2O)_2](H_2O)_{5.44}Cl\}^{\bullet}$ showing the channels along the *c*-axis. The disordered included water molecules are omitted for clarity.

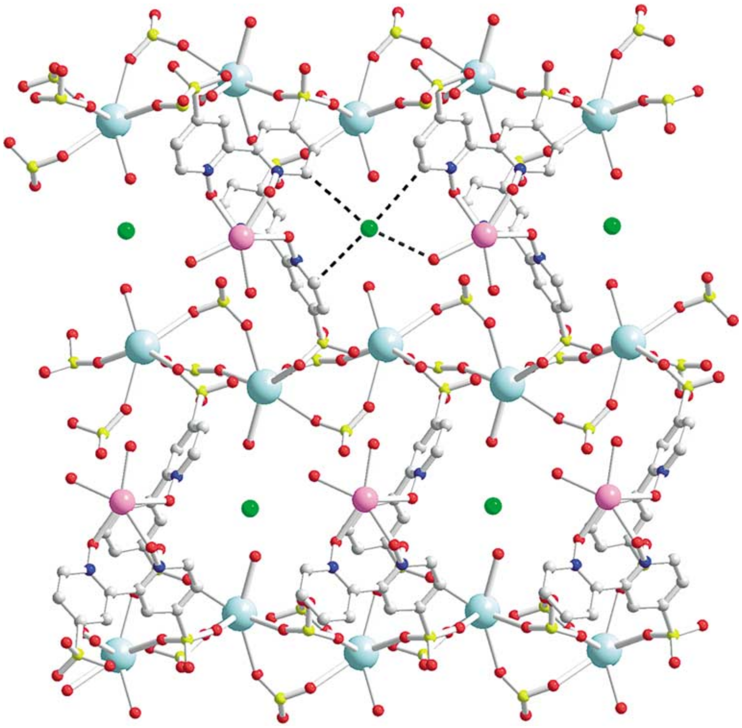

Fig. 8. $\{Ba_2(H_2O)_4[Eu4_3(H_2O)_2](H_2O)_{5.44}Cl\}^{\bullet}$ viewed slightly off the *a*-axis showing the location of $Cl^-$ ions within the 'grottos'. Dashed bonds indicate hydrogen bonding interactions.

ring. The sides of the rings are composed of $SO_3$ groups bridged by a second silver centre. The coordination sphere of this metal centre is a distorted tetrahedron containing three oxygen atoms, from three different sulfonate groups that cross-link the structure together, and a molecule of MeCN. The rings pack along the crystallographic *c*-axis in an eclipsed fashion to give channels containing the MeCN guests. The channel dimensions are 7.9(1) high by 14.6(1) Å wide as defined by the transannular Ag–Ag distances of the rings.

Upon heating $[Ag(\mathbf{5})(MeCN)_{0.5}]^{\bullet}$, no mass loss is observed until 170 °C at which point the tightly held MeCN guests are lost. The reversion to the desolvated form, $[Ag(\mathbf{5})]^{\bullet}$, is a crystal-to-crystal transformation that involves a shift from the triclinic crystal system of the solvated state to the tetragonal $[Ag(\mathbf{5})]^{\bullet}$. Remarkably, this transformation is completely reversible simply by exposing the desolvated powder to MeCN vapor despite the network requiring a major structural rearrangement. Treatment of the apohost with other nitriles, even propionitrile, MeOH, EtOH, THF, yielded no change in the observed PXRD, indicating selectivity for MeCN.

The apo-host is a dense 3D solid containing ribbons of silver ions. Stoichiometrically, only one silver ion is contained in the asymmetric unit of $[Ag(\mathbf{5})]^{\bullet}$ but is distributed over three partially occupied sites in a 2:1:1 ratio, with only one unique molecule of **5** present. Ag1 occupies 50% of the silver sites and is the only silver center which forms bonds to the N atoms of pyridyl rings. It also has two longer contacts to sulfonate oxygen atoms and two even longer contacts to two adjacent silver centres, Ag2 and symmetry related Ag1′. Ag1 and Ag2 form the ribbons of silver ions permeating through this structure, repeating in a Ag1–Ag2–Ag1 unit, with distances shorter (2.988–3.015 Å) than the sum of van der Waals radii (3.44 Å) [101–105]. Ag3 is coordinated by four equivalent sulfonate oxygen atoms. These atoms, along with the ligands, define a square surrounding each $\{Ag1–Ag2–Ag1\}^{\bullet}$ ribbon, with the two sulfonate oxygen atoms and pyridyl *N*-atoms acting as the ‘coordinating sleeve’ (Fig. 10).

The interconversion between these structures involves a redistribution of coordinative interactions about the silver cations within the structure. For coordination networks, having a structural rearrangement where the structure change involves the metal coordination sphere is quite rare [106–112]. The majority of these past examples involve a change from a discrete complex to an infinite inclusion network, and, for other cases, where a guest induced change between extended networks was observed, the selectivity and/or reversibility was not high. Notably, our system undergoes a transition that involves the greatest extent of structural rearrangement, and demonstrates the highest selectivity for guest uptake.

The mechanism for interconversion relies on the differentiation in coordination power between pyridyl *N*-donation versus sulfonate *O*-coordination. The pyridine coordination anchors the ligand to $Ag^{I}$, while the weaker sulfonate interactions are ‘mobile’ and serve to saturate the coordination sites left vacant upon removal of MeCN. Ag–sulfonate bonds participate in the bond making and bond breaking processes. Comparing the two crystal structures in Fig. 11, it can be seen, that in order to fill the void space, the rings collapse like a cardboard square by bending one side to force it into the box’s cavity. The rearrangement begins with ‘folding in’ of one of the sulfonate-ligated silver ions, the side of the square, to fill the void generated by the loss of MeCN. This silver ion now becomes proximal to the pyridine bound silver atoms. This motion requires the translation of the second, originally equivalent, sulfonate-ligated silver ions in the same direction, but out of the square and away from the collapsing void, to generate the third type of Ag center in $[Ag(\mathbf{5})]^{\bullet}$.

The factors contribute to the ability of the network to rearrange are as follows: The coordinative pliancy of the coordination sphere of $Ag^{I}$ provides a surface over which sulfonate groups can move as a ‘Ball of Velcro’, i.e. as one Ag–O linkage is compromised, a new Ag–O interaction is generated, enabling a continuum of silver ion ligation throughout the conversion event. This process was repeated 20 times with no observed broadening of peaks in PXRD pattern of the tested material. The efficient reversibility between the ordering of these two structures, triggered by MeCN uptake/loss, owes to the weak Ag–sulfonate interactions and indicates the ease with which the framework can re-organize to attain its energetic minimum. The smooth transition between structures demonstrates the flexibility of Ag–sulfonate networks, in contrast to the eventual disordering of a network in systems with stronger, more directional, bonding.

### 3.3. *Topotactic intercalation into silver triflate*

The triflate anion (trifluoromethanesulfonate, $^{-}OTf$) can be considered as the weakest of the weakly coordinating family of sulfonate ligands due to the strongly electron withdrawing effects of the $–CF_3$ moiety markedly lowering the Lewis basicity of the coordinating $–SO_3$ group ($pK_a$ HOTf $< -12$ vs. $MeSO_3H = \sim -2.5$). For these electronic reasons triflate ions have been regarded as the quintessential ‘non-coordinating’ anion in classical coordination chemistry [40].

As with other silver monosulfonates, AgOTf is also a layered material as determined by PXRD analysis which show the characteristic set of equally spaced intense Bragg reflections from the low order planes of layered solids. Surprisingly, there is no single crystal X-ray structure of AgOTf [113].[1] Since we previously determined that AgOTs was capable of intercalating nonylamine [53], we sought to also investigate the intercalation capabilities of AgOTf [114].

---

[1] AgOTf undergoes two reversible phase changes at 280 and 323 °C. This observation is indicative of the ability of the layers to reorient. We have also found that AgOTf can intercalate alkyl acetates, cyclic ethers, and nitroalkanes.

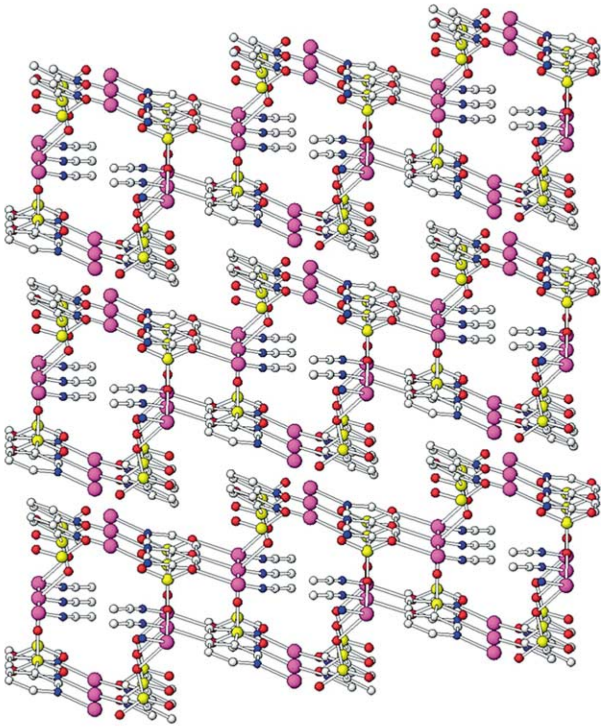

Fig. 9. View of the extended structure of $[\mathrm{Ag}(\mathbf{5})(\mathrm{MeCN})_{0.5}]^{\bullet}$ looking down the *c*-axis, showing the MeCN channels formed from the linking of the 24-membered rings.

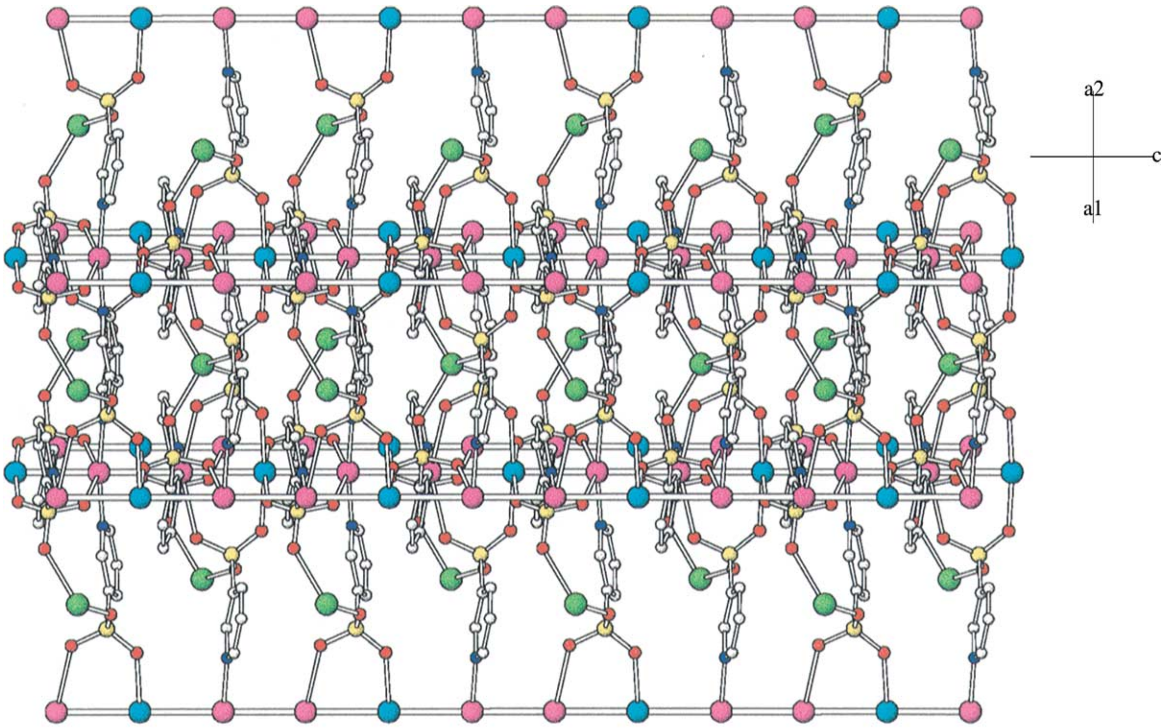

Fig. 10. View of $[\mathrm{Ag}(\mathbf{5})]^{\bullet}$ perpendicular to the *c*-axis illustrating the ribbons of Ag ions permeating the structure. Large spheres all represent silver but crystallographic equivalents are shaded differently.

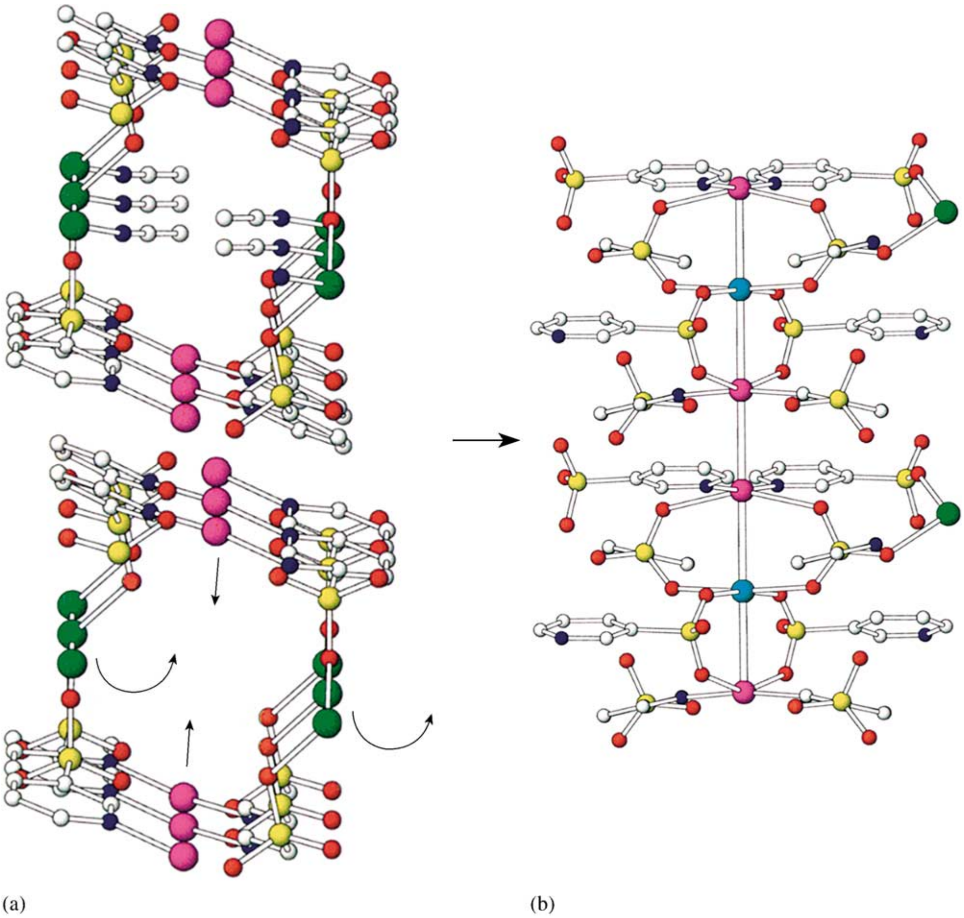

Fig. 11. Illustration of the mechanism of interconversion of (a) [Ag(**5**)(MeCN)$_{0.5}$]$^{\bullet}$ and (b) [Ag(**5**)]$^{\bullet}$. The included MeCN molecules in (a) have been artificially deleted to show the void that would exist. Large spheres all represent silver but crystallographic equivalents are shaded differently.

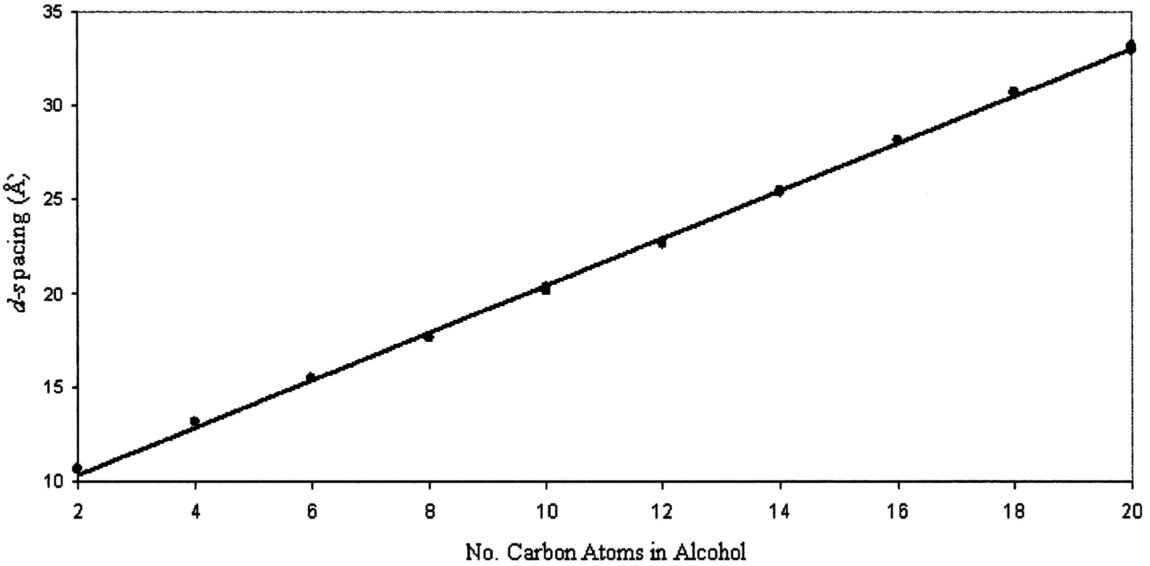

Fig. 12. Plot of $d_{001}$-spacing vs. the number of carbon atoms contained in the primary alcohols intercalated into AgOTf, demonstrating regular linear increase in layer spacing that occurs.

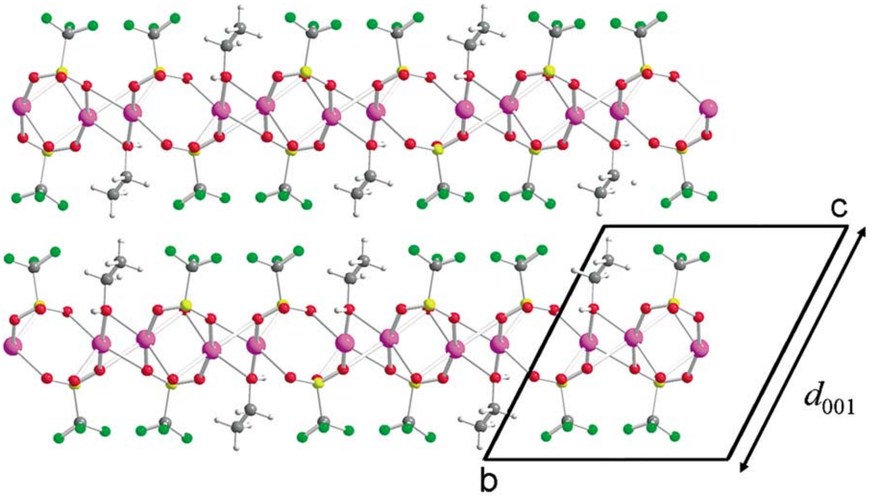

Fig. 13. View of the lamellar network from by AgOTf θ EtOH, showing the $CF_3$ and EtOH groups directed into the interlayer region.

AgOTf was exposed to a series of primary alcohols of varying chain lengths ranging from 2 to 20 carbon atoms. PXRD analysis identified these products as layered materials having a monotonic increase in the *d*-spacings for the principal (0 0 1) Bragg reflections with respect to the number of carbon atoms in the alcohol alkyl chain. This indicated that the AgOTf layers are pushed further apart by longer alcohols (Fig. 12). Thus, the reaction of a primary alcohols with AgOTf spontaneously leads to formation of a polycrystalline intercalation compound, whose interlayer spacing can be controlled by the length of the alcohol's carbon chain.

Structural characterization of the intercalates was challenging and only the crystal structure of the ethanol intercalate was attainable. The structure shows that the nature of the host–guest interaction is coordinative, with the hydroxyl oxygen of EtOH bridging two $Ag^{I}$ centers within the layer, while the ethyl and $–CF_3$ groups project into the interlayer region (Fig. 13).

To determine if the nature of the host–guest interaction for the all the intercalates was consistent, the PXRD data obtained for the rest of the intercalates was correlated with the single crystal data obtained for the EtOH intercalate. In EtOH θ AgOTf the distance between symmetry-related EtOH oxygen atoms on opposite sides of a layer following the *c*-axis is 8.22(2) Å. Summing this value with the ideal $O–C_{\text{terminal}}$ distances obtained from MM2 calculations for the other alcohols, assuming all-trans conformations, gives the distance corresponding to the (0 0 1) peaks ($d_{001}$) in the PXRD patterns for each of the intercalates (Fig. 14). From this the following may be concluded: (1) The longer

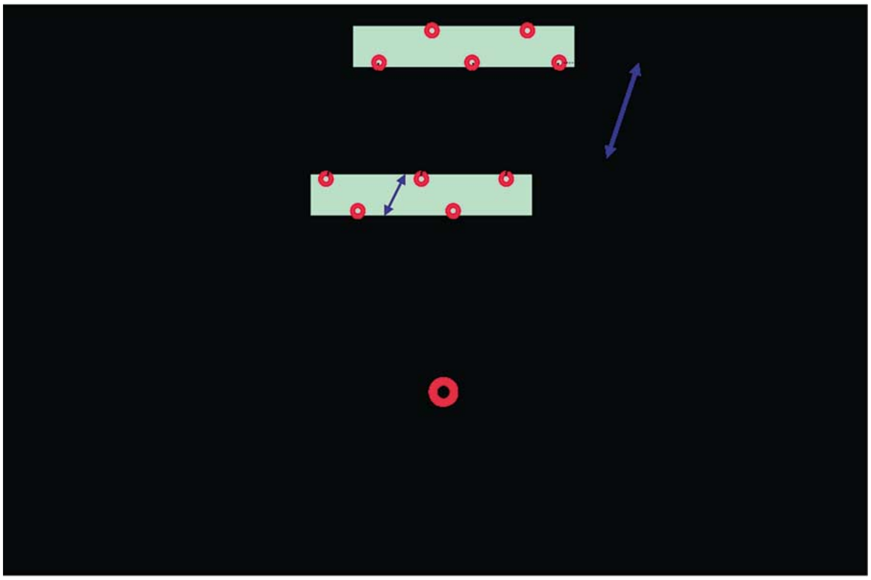

Fig. 14. Illustration of the calculation of $d_{001}$ from AgOTf θ EtOH crystallographic parameters and MM2 calculations. Note that a unit cell translation of 1/2*c* from the origin used for the determination AgOTf θ EtOH has been made for this calculation to give an integral relationship.

chained alcohols are coordinating to the Ag layers in a manner analogous to EtOH θ AgOTf; (2) The alkyl chains of the orient along an axis parallel to the *c*-axis in EtOH θ AgOTf; (3) The alcohols adopt an interdigitated rather than a bilayer arrangement within the interlayer region; (4) The intercalation of straight chained alcohols into AgOTf is topotactic.

Silver triflate can be regarded as an adaptive material, capable of rearranging its structure to accommodate a guest molecule. Jacobson and Johnson studied the intercalation of alcohols into layered vanadyl phosphonates by imprinting of binding site for alcohol coordination to the layer [115]. Poojary and Clearfield structurally determined amine intercalates of Zn phenylphosphonate [116]. However, for these systems, thermal liberation of solvent from the layer was required to generate a binding site for the intercalant molecule. Typically, this desolvated state was found to be highly moisture sensitive. In contrast, intercalates of AgOTf can be readily obtained by direct addition of a primary alcohol to commercially available salt. The layers simply re-orient to accommodate the guest. The resulting intercalates, especially those of the higher chained alcohols are not especially light or moisture sensitive at a relative humidity of ∼20–30% at 23 °C.

## 4. Summary and conclusions

Sulfonate anions are a relatively unexplored class of ligands for the construction of coordination frameworks. This has been due to the perception of the sulfonate group as being a poor ligand, incapable of forming stable coordinate bonds with metal ions. However, as we have demonstrated, not only can stable structures be formed via cooperative bonding effects using sulfonates, but these networks can also display functionality. These properties are not always attainable from more traditional classes of ligands with more rigid coordinative preferences. Moreover, the description of the sulfonate group as a ‘Ball of Velcro’, capable of breaking one interaction and generating another, without sacrificing of structural stability, lends a new concept to the design and synthesis of infinite coordination frameworks.

Recently, there has been a move to broaden the definition of the term ‘porous’ for extended solids to ‘reversible guest sorption’, rather than to limit it to only define structures that exhibit permanent porosity [117]. This new terminology would then allow for the inclusion of networks that collapse, or rearrange their connectivity, to allow for the removal and reintroduction of guest molecules to also be classified as functional materials in this sense. We believe that the use of sulfonate-based ligands as components of extended solids will play a significant role in the burgeoning area of flexible, or soft, materials [108,118–122].

## References

[1] Y. Aoyama, Top. Curr. Chem. 198 (1998) 131.
[2] T. Hertzsch, F. Budde, E. Weber, J. Hulliger, Angew. Chem. Int. Ed. Engl. 41 (2002) 2282.
[3] K. Fuji, T. Furuta, T. Otsubo, K. Tanaka, Tetrahedron Lett. 40 (1999) 3001.
[4] A.K. Cheetham, G. Férey, T. Loiseau, Angew. Chem. Int. Ed. Engl. 38 (1999) 3268.
[5] P. Sozzani, A. Comotti, R. Simonutti, T. Messmann, J.W. Logan, Angew. Chem. Int. Ed. Engl. 39 (2000) 2695.
[6] D.W. Breck, Zeolite and Molecular Sieves: Structure, Chemistry and Use, Wiley, New York, 1974.
[7] R.M. Barrer, Zeolites and Clay Minerals as Sorbents and Molecular Sieves, Academic Press, New York, 1978.
[8] M.A. Occelli, H. Robson, Expanded Clays and Other Microporous Solids, Academic Press, New York, 1992.
[9] M.S. Whittingham, Prog. Solid State Chem. 12 (1978) 41.
[10] A.J. Jacobson, in: A.K. Cheetham, P. Day (Eds.), Solid State Chemistry Compounds, Clarendon, Oxford, 1992, p. 182.
[11] G. Cao, H.-G. Hong, T.E. Mallouk, Acc. Chem. Res. 25 (1992) 420.
[12] A. Clearfield, U. Costantino, in: J.L. Atwood, J.E.D. Davies, D.D. MacNicol, F. Vögtle (Eds.), Comprehensive Supramolecular Chemistry, vol. 7, Elsevier Science, New York, 1996, p. 151.
[13] B. Moulton, M.J. Zaworotko, Chem. Rev. 101 (2001) 1629.
[14] F.A. Cotton, C. Lin, C.A. Murillo, Acc. Chem. Res. 34 (2001) 759.
[15] T.J. Barton, L.M. Bull, W.G. Luemperer, D.A. Loy, B. McEnaney, M. Misono, P.A. Monson, G. Pez, G.W. Scherer, J.C. Vartuli, O.M. Yaghi, Chem. Mater. 9 (1997) 2039.
[16] O.M. Yaghi, J. Li, C. Davis, D. Richardson, T.L. Groy, Acc. Chem. Res. 34 (1998) 474.
[17] S.R. Batten, R. Robson, Angew. Chem. Int. Ed. Engl. 37 (1998) 1460.
[18] S. Kitagawa, M. Kondo, Bull. Chem. Soc. Jpn. 71 (1998) 1739.
[19] C.L. Bowes, G.A. Ozin, Adv. Mater. 8 (1996) 13.
[20] P.J. Hagrman, D. Hagrman, J. Zubieta, Angew. Chem. Int. Ed. Engl. 38 (1999) 2639.
[21] L. Ouahab, Chem. Mater. 9 (1997) 1909.
[22] J.S. Seo, D. Whang, H. Lee, S.I. Jun, J. Oh, Y.J. Jeon, K. Kim, Nature 404 (2000) 982.
[23] J. Plevert, T.M. Gentz, A. Laine, H.L. Li, V.G. Young, O.M. Yaghi, M. O’Keeffe, J. Am. Chem. Soc. 123 (2001) 12706.
[24] S.S.Y. Chui, S.M.F. Lo, J.P.H. Charmant, A.G. Orpen, I.D. Williams, Science 283 (1999) 1148.
[25] B.L. Chen, M. Eddaoudi, S.T. Hyde, M. O’Keeffe, O.M. Yaghi, Science 291 (2001) 1021.
[26] M. Eddaoudi, H.L. Li, O.M. Yaghi, J. Am. Chem. Soc. 122 (2000) 1391.
[27] H. Li, M. Eddaoudi, M. O’Keeffe, O.M. Yaghi, Nature 402 (1999) 276.
[28] S. Noro, S. Kitagawa, M. Kondo, Angew. Chem. Int. Ed. Engl. 39 (2000) 2081.
[29] K. Seki, Chem. Commun. (2001) 1496.
[30] M. Eddaoudi, J. Kim, N. Rosi, D. Vodak, J. Wachter, M. O’Keeffe, O.M. Yaghi, Science 295 (2002) 469.
[31] G. Alberti, U. Costantiono, in: J.L. Atwood, J.E.D. Davies, D.D. MacNicol, F. Vögtle (Eds.), Comprehensive Supramolecular Chemistry, vol. 7, Elsevier Science, New York, 1996, p. 1.
[32] G. Alberti, U. Costantino, in: J.L. Atwood, J.E. Davies, D.D. MacNicol (Eds.), Inclusion Compounds, vol. 5, Oxford University Press, New York, 1991, p. 136.
[33] J.-C. Grenier, J.-M. Bassat, J.-P. Doumerc, J. Etourneau, Z. Fang, L. Fournes, S. Petit, M. Pouchard, A. Wattiaux, J. Mater. Chem. 9 (1999) 25.
[34] D.M. Kaschak, S.A. Johnson, D.E. Hooks, H.-N. Kim, M.D. Ward, T.E. Mallouk, J. Am. Chem. Soc. 120 (1998) 10887.

[35] T. Nakato, Y. Furumi, T. Okuhara, Chem. Lett. (1998) 611.
[36] Y. Santiago, C.R. Cabrera, J. Electrochem. Soc. 141 (1994) 629.
[37] S.A. Solin, Annu. Rev. Mater. Sci. 27 (1997) 89.
[38] (a) F. Leroux, M. Adachi-Pagano, M. Intissar, S. Chauveière, C. Forano, J.-P. Besse, J. Mater. Chem. 11 (2001) 105;
(b) S. Nakano, T. Sasaki, K. Takemura, M. Watanabe, Chem. Mater. 10 (1998) 2044.
[39] A. Clearfield, Prog. Inorg. Chem. 47 (1998) 371.
[40] J.A. Davies, C.A. Hockensmith, V.Y. Kukushkin, Y.N. Kukushkin, Synthetic Coordination Chemistry: Principles and Practice, World Scientific, London, 1996, p. 58.
[41] G.A. Lawrence, Chem. Rev. 86 (1986) 17.
[42] G. Smith, B.A. Cloutt, D.E. Lynch, K.A. Byriel, C.H.L. Kennard, Inorg. Chem. 37 (1998) 3236.
[43] B.J. Gunderman, P.J. Squatritto, Inorg. Chem. 34 (1995) 2399.
[44] B.J. Gunderman, P.J. Squatritto, Inorg. Chem. 33 (1994) 2924.
[45] Y. Garaud, F. Charbonnier, R. Faure, J. Appl. Crystallogr. 13 (1980) 190.
[46] B.J. Gunderman, I.D. Kabell, P.J. Squatritto, S.N. Dubey, Inorg. Chim. Acta. 258 (1992) 297.
[47] S.A. Dalrymple, M. Parvez, G.K.H. Shimizu, Chem. Commun. (2001) 2672.
[48] S.A. Dalrymple, G.K.H. Shimizu, Chem. Commun. (2002) 2224.
[49] A.L. Ardunini, M. Garnett, R.C. Thompson, T.C.T. Wong, Can. J. Chem. 53 (1975) 3812.
[50] C.S. Alleyne, K.O. Mailer, R.C. Thompson, Can. J. Chem. 52 (1973) 336.
[51] C.S. Alleyne, R.C. Thompson, Can. J. Chem. 52 (1974) 3218.
[52] J.S. Haynes, J.R. Sams, R.C. Thompson, Can. J. Chem. 59 (1980) 669.
[53] G.K.H. Shimizu, G.D. Enright, C.I. Ratcliffe, G.S. Rego, J.L. Reid, J.A. Ripmeester, Chem. Mater. 10 (1998) 3282.
[54] G.K.H. Shimizu, G.D. Enright, C.I. Ratcliffe, K.F. Preston, J.L. Reid, J.A. Ripmeester, Chem. Commun. (1999) 1485.
[55] J.-M. Lehn, Supramolecular Chemistry, Concepts and Perspectives, VCH, Weinheim, 1995.
[56] S.K. Mäkinen, N.J. Melcer, M. Parvez, G.K.H. Shimizu, Chem. Eur. J. 7 (2001) 5176.
[57] C.H. Chen, J.W. Cai, X.L. Feng, X.M. Chen, J. Chem. Crystallogr. 31 (2001) 271.
[58] J.W. Cai, C.H. Chen, X.L. Feng, C.Z. Liao, X.M. Chen, J. Chem. Soc. Dalton Trans. (2001) 2370.
[59] J.W. Cai, C.H. Chen, C.Z. Liao, X.L. Feng, X.M. Chen, Acta Crystallogr. Sect. B 57 (2001) 520.
[60] J.W. Cai, C.H. Chen, C.Z. Liao, J.H. Yao, X.P. Hu, X.M. Chen, J. Chem. Soc. Dalton Trans. (2001) 1137.
[61] C.H. Chen, J.W. Cai, C.Z. Liao, X.L. Feng, X.M. Chen, S.W. Ng, Inorg. Chem. 41 (2002) 4967.
[62] A.W. Coleman, S.G. Bott, S.D. Morley, C.M. Means, K.D. Robinson, H. Zhang, J.L. Atwood, Angew. Chem. Int. Ed. Engl. 27 (1988) 1361.
[63] G.W. Orr, L.J. Barbour, J.L. Atwood, Science 285 (1999) 1049.
[64] C.P. Johnson, J.L. Atwood, J.W. Steed, C.B. Bauer, R.D. Rogers, Inorg. Chem. 35 (1996) 2602.
[65] J.L. Atwood, G.W. Orr, N.C. Means, F. Hamada, H.M. Zhang, S.G. Bott, K.D. Robinson, Inorg. Chem. 31 (1992) 603.
[66] H.R. Webb, M.J. Hardie, C.L. Raston, Chem. Eur. J. 7 (2001) 3616.
[67] S.J. Dalgarno SJ, C.L. Raston, Chem. Commun. (2002) 2216.
[68] M.J. Hardie, J.A. Johnson, C.L. Raston, H.R. Webb, Chem. Commun. (2000) 849.
[69] J.L. Atwood, L.J. Barbour, M.J. Hardie, C.L. Raston, Coord. Chem. Rev. 222 (2001) 3.
[70] R.D. Shannon, Acta Crystallogr. Sect. A 32 (1976) 751.
[71] A.P. Côté, G.K.H. Shimizu, Chem. Commun. (2001) 251.
[72] M.B. Dines, P.M. DiGiacomo, P.C. Griffith, R.H. Lane, R.E. Cooksey, in: J.S. Miller (Ed.), Chemically Modified Surfaces in Catalysis and Electrocatalysis. ACS Symp. Ser. 192, American Chemical Society, Washington, DC, 1982, p. 223.
[73] D.M. Poojary, P.C. Bellinghausen, B. Zhang, A. Clearfield, Inorg. Chem. 35 (1996) 4942.
[74] B. Zhang, D.M. Poorjary, A. Clearfield, Inorg. Chem. 37 (1998) 1844.
[75] F. Charbonnier, R. Faure, H. Loisleur, Acta Crystallogr. Sect. B 37 (1981) 822.
[76] R.S.K.A. Gamage, B.M. Peake, J. Simpson, Aust. J. Chem. 46 (1993) 1595.
[77] A. Koeberg-Telder, H. Cerfontain, C.H. Stam, G. Kreuning, Recl. Trav. Chim. Pays-Bas 106 (1987) 142.
[78] A.P. Côté, G.K.H. Shimizu, Unpublished results.
[79] S.A. Dalrymple, G.K.H. Shimizu, Chem. Eur. J. 8 (2002) 3010.
[80] L.A. Vermeulen, J.L. Snover, L.S. Sapochak, M.E. Thompson, J. Am. Chem. Soc. 115 (1993) 11767.
[81] L.A. Vermeulen, M.E. Thompson, Nature 358 (1992) 656.
[82] O.M. Yaghi, H. Li, J. Am. Chem. Soc. 118 (1996) 295.
[83] O.M. Yaghi, H. Li, T.L. Groy, Inorg. Chem. 36 (1997) 4292.
[84] G.K.H. Shimizu, G.D. Enright, C.I. Ratcliffe, J.A. Ripmeester, Chem. Commun. (1999) 1379.
[85] B. Sui, J. Fan, T. Okamura, W.-Y. Sun, N. Ueyama, New J. Chem. 25 (2001) 1379.
[86] O.S. Jung, Y.J. Kim, Y.-A. Lee, H.K. Chae, H.G. Jang, J. Hong, Inorg. Chem. 40 (2001) 2105.
[87] K.S. Min, M.P. Suh, J. Am. Chem. Soc. 122 (2000) 6834.
[88] S.K. Sharma, C.E. Snyder Jr, L.J. Gschwender, Lubr. Eng. 55 (1999) 27.
[89] J.O. Yu, A.P. Côté, G.D. Enright, G.K.H. Shimizu, Inorg. Chem. 40 (2001) 582.
[90] D. Venkataraman, Y. Du, S.R. Wilson, P. Zhang, K. Hirsch, J.S. Moore, J. Chem. Ed. 74 (1997) 915.
[91] B.D. Chandler, A.P. Côté, D.T. Cramb, J.M. Hill, G.K.H. Shimizu, Chem. Commun. (2002) 1900.
[92] L. Ma, O.R. Evans, B.M. Foxman, W.B. Lin, Inorg. Chem. 38 (1999) 5837.
[93] C. Seward, N.X. Hu, S. Wang, J. Chem. Soc. Dalton Trans. (2001) 134.
[94] J.-C.G. Bünzli, C. Piguet, Chem. Rev. 102 (2002) 1897.
[95] C. Serre, F. Millange, J. Marrot, G. Férey, Chem. Mater. 14 (2002) 2409.
[96] S. Ktagawa, S. Matsuyama, M. Munakata, T. Emori, J. Chem. Soc. Dalton Trans. (1991) 2869.
[97] L.M. Englehardt, C. Pakawatchai, A.H. White, P.C. Healy, J. Chem. Soc. Dalton Trans. (1985) 117.
[98] H. Adams, N.A. Bailey, D.W. Bruce, S.C. Davis, D.A. Dunmur, P.D. Hempstead, S.A. Hudson, S. Thorpe, J. Mater. Chem. 2 (1992) 395.
[99] T. Suzuki, H. Katsuki, K. Isobe, N. Moriya, Y. Nakagawa, M. Ochi, Inorg. Chem. 34 (1995) 530.
[100] F. Jaber, F. Charbonnier, R. Faure, M. Petit-Ramel, Z. Kristallogr. 209 (1994) 536.
[101] Q.M. Wang, T.C.W. Mak, J. Am. Chem. Soc. 123 (2001) 1501.
[102] Q.M. Wang, T.C.W. Mak, Angew. Chem. Int. Ed. Engl. 40 (2001) 1407.
[103] M.A. Rawashdeh-Omary, M.A. Omary, H.H. Patterson, J. Am. Chem. Soc. 122 (2000) 10371.
[104] M.A. Omary, T.R. Webb, Z. Assefa, G.E. Shankle, H.H. Patterson, Inorg. Chem. 37 (1998) 1380.
[105] C.M. Che, M.C. Tse, M.C.W. Chan, K.K. Phillips, K.H. Leung, J. Am. Chem. Soc. 122 (2000) 2464.
[106] E. Cariati, X. Bu, P.C. Ford, Chem. Mater. 12 (2000) 3385.
[107] L.G. Beauvais, M.P. Shores, J.R. Long, J. Am. Chem. Soc. 122 (2000) 2763.
[108] D.V. Soldatov, J.A. Ripmeester, S.I. Sherigin, I.E. Sokolov, A.S. Zanina, S.A. Gromilov, A. Dyadin, J. Am. Chem. Soc. 121 (1999) 4179.

[109] D.V. Soldatov, J.A. Ripmeester, Chem. Mater. 12 (2000) 1827.
[110] B.O. Patrick, W.M. Reiff, V. Sanchez, A. Storr, R.C. Thompson, Polyhedron 20 (2001) 1577.
[111] L. Carlucci, G. Ciani, D.W. v. Gudenberg, D.M. Proserpio, New J. Chem. 23 (1999) 397.
[112] O. Kahn, J. Larionova, J.V. Yahkmi, Chem. Eur. J. 5 (1999) 3433.
[113] A.P. Côté, G.K.H. Shimizu, Unpublished results.
[114] A.P. Côté, M.J. Ferguson, K.A. Khan, G.D. Enright, A.D. Kulynych, S.A. Dalrymple, G.K.H. Shimizu, Inorg. Chem. 41 (2002) 287.
[115] G. Huan, A.J. Jacobson, J.W. Johnson, E.W. Cocoran Jr, Chem. Mater. 2 (1990) 91.
[116] D.M. Poojary, A. Clearfield, J. Am. Chem. Soc. 117 (1995) 11278.
[117] O.M. Yaghi, M. O’Keeffe, M. Kanatzidis, J. Solid State Chem. 152 (2000) 1.
[118] R. Kitaura, K. Fujimoto, S.-I. Noro, M. Kondo, S. Kitagawa, Angew. Chem. Int. Ed. Engl. 41 (2002) 149.
[119] K. Biradha, Y. Hongo, M. Fujita, Angew. Chem. Int. Ed. Engl. 41 (2002) 3395.
[120] K. Biradha, M. Fujita, Angew. Chem. Int. Ed. Engl. 41 (2002) 3392.
[121] L.C. Tabares, J.A.R. Navarro, J.M. Salas, J. Am. Chem. Soc. 123 (2001) 383.
[122] K. Uemura, S. Kitagawa, M. Kondo, K. Fukui, R. Kitaura, H.-C. Chang, T. Mizutani, Chem. Eur. J. 8 (2002) 3587.